

Modal analysis on quantum computers via qubitization

Yasunori Lee* and Keita Kanno†

QunaSys, Bunkyo, Tokyo, Japan

Natural frequencies and normal modes are basic properties of a structure which play important roles in analyses of its vibrational characteristics. As their computation reduces to solving eigenvalue problems, it is a natural arena for application of quantum phase estimation algorithms, in particular for large systems. In this note, we take up some simple examples of (classical) coupled oscillators and show how the algorithm works by using qubitization methods based on a sparse structure of the matrix. We explicitly construct block-encoding oracles along the way, propose a way to prepare initial states, and briefly touch on a more generic oracle construction for systems with repetitive structure. As a demonstration, we also give rough estimates of the necessary number of physical qubits and actual runtime it takes when carried out on a fault-tolerant quantum computer.

* lee.y@qunasys.com

† kanno@qunasys.com

Contents

1	Introduction and Summary	1
2	Review of qubitization of sparse matrices	3
2.1	Block encoding	4
2.2	Qubitization	6
3	Application to modal analysis	7
3.1	Settings	7
3.2	Adder	8
3.3	Oracle O_F	9
3.4	Oracle O_H	10
3.5	Example 1: equal spring constants	12
3.6	Example 2: alternating spring constants	14
3.7	Generalization: multiple layers	17
4	Initial states and their preparation	18
4.1	Proposal	18
4.2	Numerical experiments	19
5	Resource estimation	21
5.1	Encoding	21
5.2	Realization of Toffoli gates	22
5.3	Case study	23
A	Quantum arithmetic and related operations	25
A.1	Adder	25
A.2	Controlled unitaries	27
A.3	Multi-controlled unitaries	28
A.4	SWAP	28
B	Speedrun	29

1 Introduction and Summary

The ultimate target of quantum computation is to solve problems which are practically intractable by classical computation due to their size and/or computational time. Among these problems is computing eigenvalues of a large matrix, where there is a quantum algorithm called the *quantum phase estimation* (QPE) [Kit95, CEMM97] which is exponentially efficient compared to any known classical algorithms (e.g. conjugate gradient method) in terms of both space and time (gate) complexity.¹ This task is of great importance as it covers a vast range of applications, including in particular quantum chemistry/physics problems of computing the energy of large systems given their Hamiltonians.

To figure out whether the desired QPE can *actually* be carried out within reasonable time, one must go beyond asymptotic scaling and estimate concrete numbers of qubits and quantum gates (especially non-Clifford ones) needed to implement the algorithm in a fault-tolerant manner. To the authors' knowledge, the program along this line was initiated in a full-fledged form by [RWS⁺16], employing *Lie-Trotter-Suzuki decomposition* and resulting in costs small enough to raise hopes but motivating further reductions. In the past few years, a novel powerful method called *qubitization* [LC16] has been developed, and utilizing it significantly reduced the number of necessary non-Clifford gates (at the expense of a moderate number of qubits), see e.g. [BGB⁺18, BGM⁺19, vBLH⁺20, LBG⁺20, KLP⁺21, SBW⁺21, GWL⁺22, DCdR⁺22, BCC⁺22, ISH⁺22, YOS⁺22, BMT⁺22, RBM⁺23, ZDdR⁺23]. At the time of writing, however, almost all the literature on application of qubitization-based QPEs has focused on quantum chemistry/physics problems, relying on decomposition of a target matrix (i.e. Hamiltonian) into a linear combination of unitaries (LCU).

In this note, we take up yet another important class of eigenvalue problems, namely *modal analysis*, and see how quantum phase estimation algorithms can be applied for toy problems of (classical) coupled oscillators. Modal analysis is important since the knowledge of natural frequencies and normal modes of a structure is indispensable to avoid unwanted resonances leading to collapses or failures, which makes it appear in various engineering scenes [Ans]. Notably, in the simplest cases, analyses reduce to eigenvalue problems of a sparse matrix, and thus one can draw on qubitization relying not on a decomposition into LCU but on

¹ Strictly speaking, one needs to prepare a suitable initial quantum state to compute a *specific* eigenvalue, which in general cannot be done efficiently and ruins the exponential advantage. Here we assume that a desirable initial state can be easily prepared, which is the case for the problems in this note (\rightarrow Sec. 4).

a sparse structure of the matrix, which gives them a somewhat different flavor compared to the existing analyses.² Although there are some previous studies [CLVBY22, SCC23] which seem to be in a similar vein at first sight, their approach is top-down and motivated by generic well-structured matrices themselves, while our work is bottom-up and more problem-oriented, which makes the direction orthogonal to some extent. The toy problems themselves are quite trivial and would provide hardly any practical benefit, but the resource estimation at least confirms the exponential advantage of quantum computation over its classical counterpart, and the authors hope that this work would serve as a step toward analyses of realistic uses in more generality: For example, the oracle construction introduced in this note can be applied to efficient simulations of exponentially many coupled oscillators described by [BBK⁺23].

The rest of the note is organized as follows. In Section 2, we give a brief overview of how to block-encode a generic sparse matrix into a unitary matrix and how to *qubitize* it. In Section 3, we consider concrete models of (classical) coupled oscillators and explicitly construct the unitary in terms of quantum circuits, starting from those of underlying oracles. In Section 4, we propose a way to prepare the input initial state of a QPE algorithm. Finally in Section 5, we roughly estimate total resources required to carry out the desired QPE. Appendix A provides elementary-gate-level implementations of various circuit components appearing in the main part.

Note added

After the first version of this work appeared on arXiv, Christoph Sünderhauf kindly informed us that the method of [SCC23] is actually applicable to our toy problems and achieves a considerable reduction in necessary resources compared to our naive circuit implementation in Sec. 3. In Appendix B, we present a further-improved implementation inspired by this finding.

² This should not be confused with so-called *sparse qubitization* which is actually LCU-based qubitization, where the (part of) original Hamiltonian is made “sparse” by truncating small coefficients.

2 Review of qubitization of sparse matrices

The problem of interest here is to compute the eigenvalues λ of a given $N \times N$ Hermitian matrix H . In order to feed the matrix H to a quantum computer, one has to somehow embed it in a unitary matrix U_H . One naive embedding is just to take $U_H = e^{icH}$ where c is some constant. Although this is conceptually simple, actual implementation as a quantum circuit is often costly, making its practical use prohibitive.

There is another embedding called *block encoding* where U_H is an $(N + \Delta N) \times (N + \Delta N)$ unitary matrix and is reduced to (suitably rescaled) H using a certain *state* vector $|\psi\rangle$ of size ΔN as

$$\langle\psi|U_H|\psi\rangle = H.$$

This type of embedding is obviously not unique, and it turns out [LC16] that among them is an especially nice one U_H^* such that

$$U_H^* \left(\frac{|\lambda\rangle|\psi\rangle \pm i|\text{orthogonal}\rangle}{\sqrt{2}} \right) = e^{\mp i \arccos \lambda} \left(\frac{|\lambda\rangle|\psi\rangle \pm i|\text{orthogonal}\rangle}{\sqrt{2}} \right) \quad (2.1)$$

where $H|\lambda\rangle = \lambda|\lambda\rangle$ and $\langle\psi|\langle\lambda|\text{orthogonal}\rangle = 0$. *Qubitization* is a method to generate U_H^* from a block encoding U_H , and by applying QPE to U_H^* , one can extract the desired information on λ with far fewer computational costs compared to the naive embedding.

Fortunately, systematic ways of (efficient) block encoding are known for several types of matrices with special properties or structures. Previous studies on cost estimation have mostly taken up those with representations in a linear combination of unitaries, appearing in quantum chemistry/physics problems e.g. as a result of Jordan-Wigner transformation of underlying fermionic Hamiltonians. However, there is another nice class of matrices with such systematic block encoding, namely *d-sparse* matrices³ with at most d non-zero entries in each row (and/or column).⁴ In the following, we introduce two special oracles O_F, O_H and review how the block encoding and the qubitization for *d-sparse* matrices are realized using them.

³ Here we follow [LC16] and adopt the symbol d (presumably after *density*).

⁴ Of course one can call any $N \times N$ matrix “ N -sparse,” but the computational advantage arises only for sparse enough matrices i.e. $d \ll N$. (The same is true for the case of LCU; any matrix can be written in a form of $\sum_i \alpha_i U_i$, but the whole algorithm can be carried out efficiently only for those with small $\|\vec{\alpha}\|$.)

2.1 Block encoding

One way to block-encode an $N \times N$ Hermitian matrix H is by using two oracles O_F and O_H [BC09, LC16] (see also [GSLW18, Lem. 48]) such that for $x \in \{1, \dots, N\}$ and $i \in \{1, \dots, d\}$,

$$O_F |x, i\rangle = |x, y_i\rangle$$

where $y_i \in \{1, \dots, N\}$ is the position (i.e. column index) of the i -th non-zero element in the x -th row, and for $x, y \in \{1, \dots, N\}$,

$$O_H |x, y\rangle |z\rangle = |x, y\rangle |z \oplus H_{xy}\rangle$$

where (z is any number and) H_{xy} is the (x, y) -element of H , hereafter assumed to be (real) non-negative,⁵ and \oplus denotes a bitwise XOR.

Let a_1, a_2 denote ancillary single-qubit registers and a_s, s denote ancillary and signal $\lceil \log_2 N \rceil$ -qubit registers respectively. Our initial target is a unitary operator

$$U_H = U_2^\dagger U_1$$

where two unitaries U_1, U_2 are such that

$$\begin{aligned} U_1 |0\rangle_{a_1} |0\rangle_{a_2} |0\rangle_{a_s} |x'\rangle_s &= \frac{1}{\sqrt{d}} \sum_{y'} \left(\sqrt{\frac{H_{x'y'}}{\max_{i,j} H_{ij}}} |0\rangle_{a_1} + \sqrt{1 - \frac{H_{x'y'}}{\max_{i,j} H_{ij}}} |1\rangle_{a_1} \right) |0\rangle_{a_2} |y'\rangle_{a_s} |x'\rangle_s \\ U_2 |0\rangle_{a_1} |0\rangle_{a_2} |0\rangle_{a_s} |x\rangle_s &= |0\rangle_{a_1} \frac{1}{\sqrt{d}} \sum_y \left(\sqrt{\frac{H_{xy}}{\max_{i,j} H_{ij}}} |0\rangle_{a_2} + \sqrt{1 - \frac{H_{xy}}{\max_{i,j} H_{ij}}} |1\rangle_{a_2} \right) |x\rangle_{a_s} |y\rangle_s \end{aligned} \quad (2.2)$$

and the summations are over y (resp. y') whose corresponding matrix elements H_{xy} (resp. $H_{x'y'}$) are non-zero. This unitary U_H block-encodes the original matrix H as

$$\langle 0|_{a_1} \langle 0|_{a_2} \langle 0|_{a_s} \langle x|_s U_H |0\rangle_{a_1} |0\rangle_{a_2} |0\rangle_{a_s} |x'\rangle_s = \frac{1}{d \cdot \max_{i,j} H_{ij}} \sum_y \sum_{y'} \underbrace{\sqrt{H_{xy} H_{x'y'}}}_{=H_{xx'}} \langle x|y'\rangle \langle y|x'\rangle$$

i.e. $\langle 0|_{a_1} \langle 0|_{a_2} \langle 0|_{a_s} U_H |0\rangle_{a_1} |0\rangle_{a_2} |0\rangle_{a_s} \sim H$.

⁵ The restriction is to avoid subtleties regarding signs and phases arising from the square roots in Eq. (2.2); for a completely general treatment, see [BC09, Sec. III]. This indeed holds for the examples in Sec. 3.

Starting from a state $|0\rangle_{a_1} |0\rangle_{a_2} |0\rangle_{a_s} |x'\rangle_s |0\rangle_v$ with an additional register v of suitable size, one can easily verify that U_1 can be realized for example by sequentially acting

1. *diffusion* gates (e.g. Hadamard gates $H^{\otimes \log_2 d}$ when d is a power of two), making an equal-superposition state $\frac{1}{\sqrt{d}} \sum_{i=1}^d |0\rangle_{a_1} |0\rangle_{a_2} |x', i\rangle_{s, a_s} |0\rangle_v$,
2. O_F , turning the state into $\frac{1}{\sqrt{d}} \sum_{i=1}^d |0\rangle_{a_1} |0\rangle_{a_2} |x', y'_i\rangle_{s, a_s} |0\rangle_v$,
3. O_H , loading the values of matrix elements as $\frac{1}{\sqrt{d}} \sum_{i=1}^d |0\rangle_{a_1} |0\rangle_{a_2} |x', y'_i\rangle_{s, a_s} |H_{x'y'_i}\rangle_v$,
4. a controlled rotation, leading to $\frac{1}{\sqrt{d}} \sum_{y'} \left(\sqrt{\frac{H_{x'y'}}{\max_{i,j} H_{ij}}} |0\rangle_{a_1} + \sqrt{1 - \frac{H_{x'y'}}{\max_{i,j} H_{ij}}} |1\rangle_{a_1} \right) |0\rangle_{a_2} |x', y'\rangle_{s, a_s} |H_{x'y'}\rangle_v$,
5. O_H again, uncomputing the state and returning the v register to $|0\rangle_v$ (as $k \oplus k = 0$ holds for any integer k), and thus achieving the desired state as in Eq. (2.2).

Note that the controlled rotation can actually be done *in-place*, making the v register unnecessary and simplifying Step 3–5. Similarly, starting from a state $|0\rangle_{a_1} |0\rangle_{a_2} |0\rangle_{a_s} |x\rangle_s |0\rangle_v$, one can check that U_2 can be realized by sequentially acting

1. diffusion gates, making an equal-superposition state $\frac{1}{\sqrt{d}} \sum_{i=1}^d |0\rangle_{a_1} |0\rangle_{a_2} |x, i\rangle_{s, a_s} |0\rangle_v$,
2. O_F , turning the state into $\frac{1}{\sqrt{d}} \sum_{i=1}^d |0\rangle_{a_1} |0\rangle_{a_2} |x, y_i\rangle_{s, a_s} |0\rangle_v$,
3. O_H , loading the values of matrix elements as $\frac{1}{\sqrt{d}} \sum_{i=1}^d |0\rangle_{a_1} |0\rangle_{a_2} |x, y_i\rangle_{s, a_s} |H_{xy_i}\rangle_v$,
4. a controlled rotation, leading to $|0\rangle_{a_1} \frac{1}{\sqrt{d}} \sum_y \left(\sqrt{\frac{H_{xy}}{\max_{i,j} H_{ij}}} |0\rangle_{a_2} + \sqrt{1 - \frac{H_{xy}}{\max_{i,j} H_{ij}}} |1\rangle_{a_2} \right) |x, y\rangle_{s, a_s} |H_{xy}\rangle_v$,
5. O_H again, uncomputing the state,
6. SWAP gates swapping a_s and s registers, achieving the desired state as in Eq. (2.2),

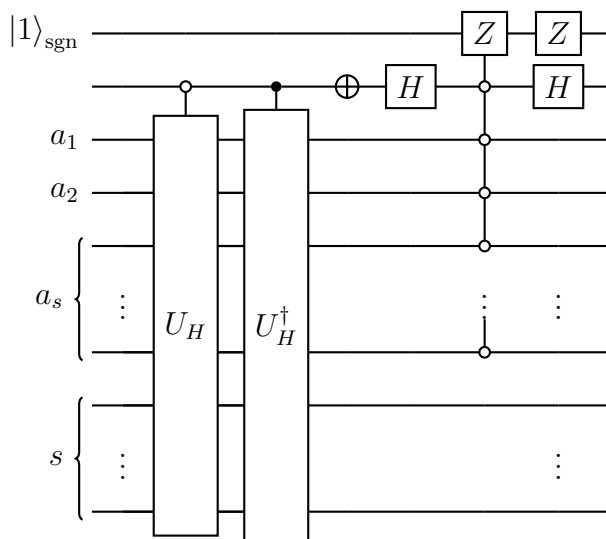
the only difference to U_1 being (which qubit to rotate and) the additional swaps at the end.

2.2 Qubitization

With the unitary U_H thus constructed at hand, one can generate a nice block encoding U_H^* called the *walk* or *iterate* operator. Following [LC16, Lem. 10], let us add another qubit and consider a unitary $\tilde{U} := |0\rangle\langle 0| \otimes U_H + |1\rangle\langle 1| \otimes U_H^\dagger$. Together with a NOT operation on the additional qubit $X := (|0\rangle\langle 1| + |1\rangle\langle 0|) \otimes I_a \otimes I_s$, the unitary U_H^* is defined to be

$$U_H^* := \left(2|+\rangle\langle +| \otimes |0\rangle_{a_1}\langle 0| \otimes |0\rangle_{a_2}\langle 0| \otimes \dots \otimes |0\rangle_{a_s}\langle 0| \otimes I_s - I \otimes I_a \otimes I_s \right) X \tilde{U}$$

which can be realized as



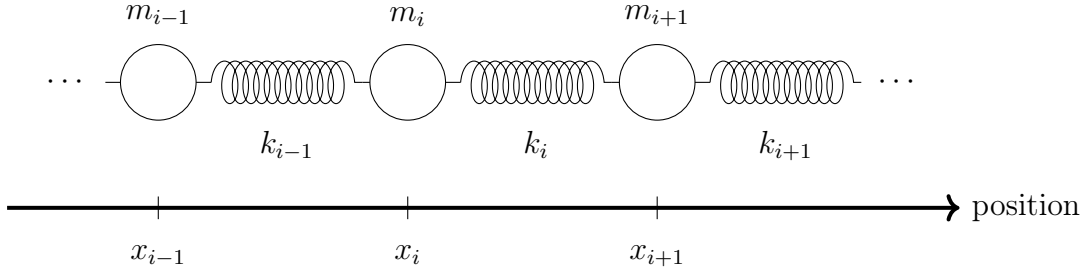
with yet another qubit (at the top in the circuit diagram) identifying a potential sign flip resulting from the reflection operation. Recalling Eq. (2.1), one can then carry out an ordinary QPE against this unitary to compute the phase $\arccos \lambda$, from which the desired eigenvalue λ of the original Hermitian matrix H can be immediately extracted.

3 Application to modal analysis

Armed with the theory of qubitization, let us see how it is actually worked out. The target is a system of coupled oscillators with which we are very familiar as a basic model of various phenomena in Nature. As will be shown below, the analyses often involve solving eigenvalue problems of sparse matrices, and thus is within a scope of the method introduced in the previous section. For the sake of simplicity, we always take the matrix size to be $N = 2^n$.

3.1 Settings

We will be considering a system of $N = 2^n$ point masses, linearly (i.e. in one dimension) and periodically connected by springs:



Here, m_i 's denote masses and k_i 's denote spring constants. The equation of motion for the i -th mass reads

$$m_i \ddot{x}_i = k_i(x_{i+1} - x_i) - k_{i-1}(x_i - x_{i-1})$$

(with $x_0 := x_N$ and $x_{N+1} := x_1$ etc.), and the natural frequencies (resp. normal modes) are given as eigenvalues (resp. eigenvectors) of an $N \times N$ matrix

$$H^{\text{original}} = \begin{pmatrix} -\frac{k_N+k_1}{m_1} & \frac{k_1}{m_1} & 0 & \dots & 0 & \frac{k_N}{m_1} \\ \frac{k_1}{m_2} & -\frac{k_1+k_2}{m_2} & \frac{k_2}{m_2} & 0 & \dots & 0 \\ 0 & \frac{k_2}{m_3} & -\frac{k_2+k_3}{m_3} & & & \vdots \\ \vdots & & & \ddots & & 0 \\ 0 & & & & -\frac{k_{N-2}+k_{N-1}}{m_{N-1}} & \frac{k_{N-1}}{m_{N-1}} \\ \frac{k_N}{m_N} & 0 & \dots & 0 & \frac{k_{N-1}}{m_N} & -\frac{k_{N-1}+k_N}{m_N} \end{pmatrix}. \quad (3.1)$$

For the toy problems examined in this note, we restrict ourselves to matrices (3.1) whose diagonal elements are all equal. This allows us to completely separate the diagonal part and the off-diagonal part and to forget about the former. As a result, target matrices H 's we want to diagonalize are 2-sparse (i.e. $d = 2$) with very simple structure, namely

$$H_{xy} \begin{cases} \neq 0 & (|x - y| = 1 \bmod 2^n), \\ = 0 & (\text{otherwise}). \end{cases} \quad (3.2)$$

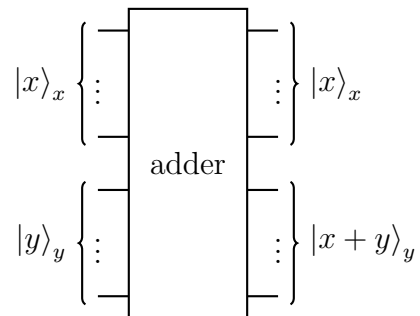
Note that these simplicities are just for demonstration; our methods can be easily generalized to treat matrices with e.g.

- non-identical diagonal elements
- non-periodic boundary conditions
- wider “band” (which in particular incorporate $k (\geq 2)$ -dimensional cases with more complicated couplings between multiple coordinates described by $kN \times kN$ matrices)

as will be described along the way.

3.2 Adder

One of the fundamental components in implementation of the oracles O_F, O_H is an adder. Given two states $|x\rangle, |y\rangle$ encoding (binary representations of) integers x, y modulo 2^n in a computational basis, the (required) function of the adder is to return a state $|x + y\rangle$ encoding $(x + y)$ modulo 2^n . In this note, we adopt the adder proposed by [CDKM04], whose I/O is schematically represented as follows



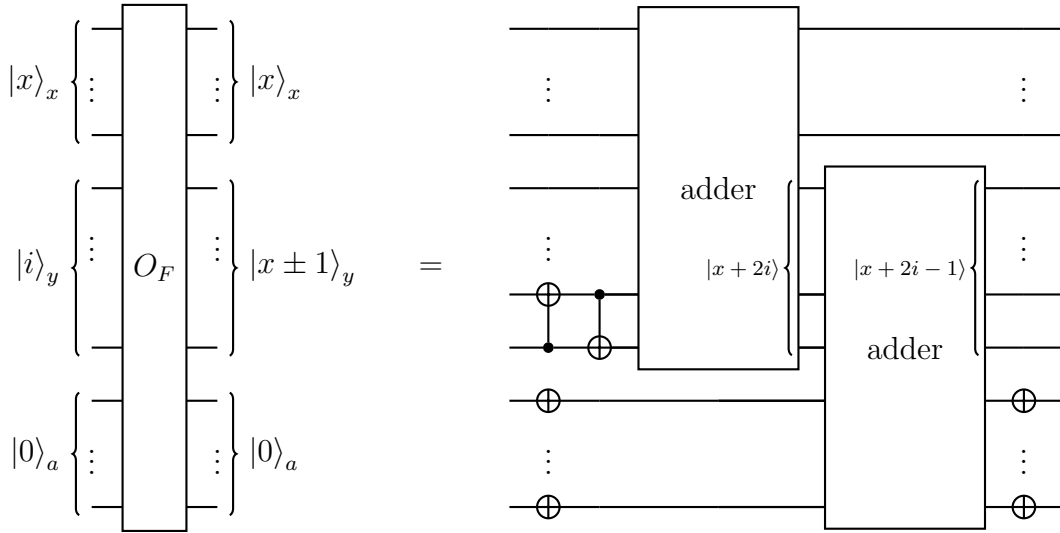
and consumes $2n$ Toffoli gates (plus a single ancillary qubit which is omitted above). For the details of implementation, see Appendix A.1.

3.3 Oracle O_F

For the matrices (3.2), non-trivial computations involving the oracle O_F are limited to⁶

$$\begin{aligned} O_F |x, 0\rangle &= |x, x - 1\rangle, \\ O_F |x, 1\rangle &= |x, x + 1\rangle. \end{aligned}$$

Recalling that flipping all bits of an integer y leads to $(2^n - 1) - y \equiv (-y - 1)$ modulo 2^n , this O_F can be implemented in a rather straightforward manner employing suitable ancillary qubits encoding “ -1 ” as



with each register x, y, a consisting of n qubits. Here, the two CNOT gates in front of the first adder *doubles* the input i , mapping $|i = 0\rangle_y \mapsto |0\rangle_y$ and $|i = 1\rangle_y \mapsto |2\rangle_y$, respectively.⁷ Also, note that the results of the addition are always output to the y register, meaning in particular that the second adder is placed “upside down.”

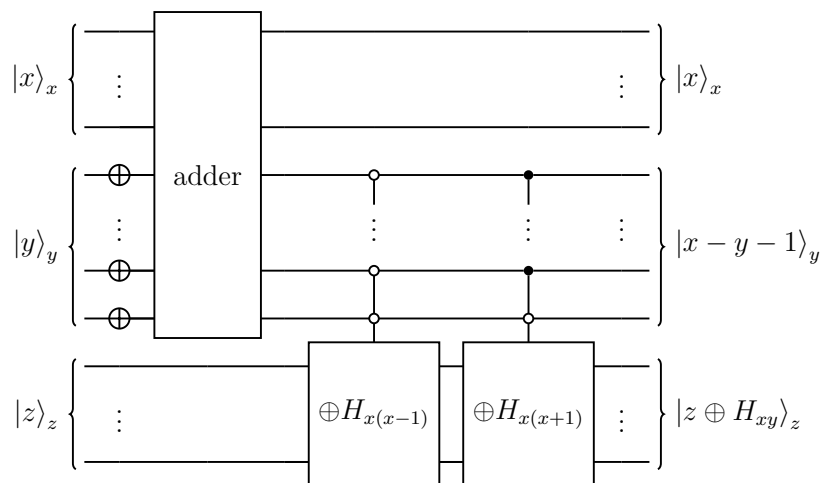
Since it contains two adders of n -bit integers, the circuit as a whole consumes $2 \times 2n = 4n$ Toffoli gates with $(3n + 1)$ qubits, where the second adder recycles the ancillary qubit of the first adder (which is omitted in the diagram).

⁶ The index origin is (shifted by one from the expressions in Sec. 2 and) set to zero for convenience.

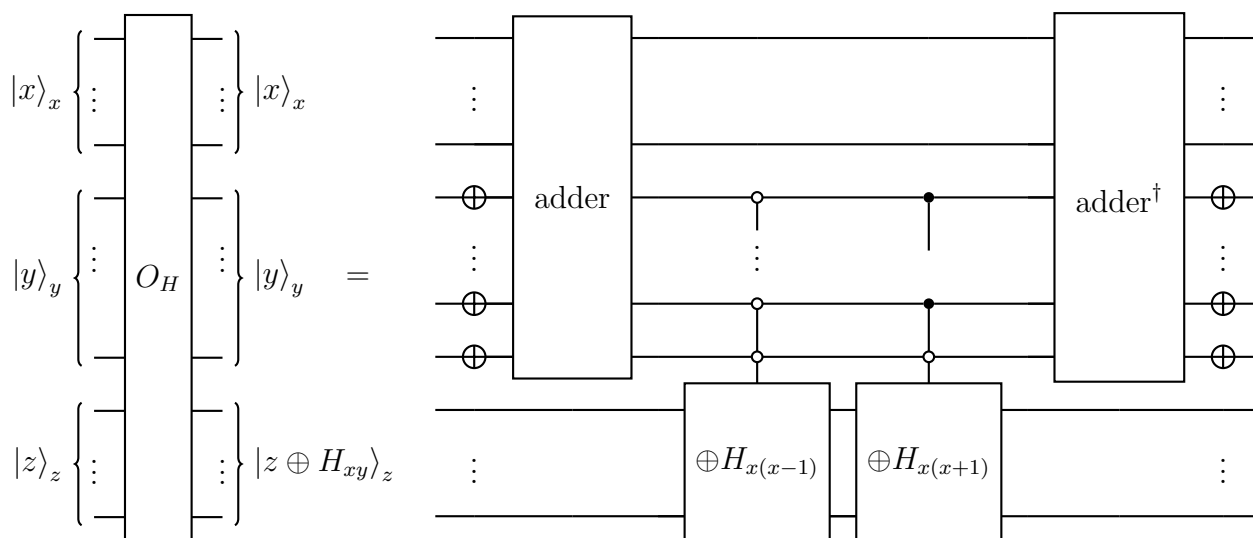
⁷ In general, one can use another qubit to first somehow check whether $0 \leq i \leq d - 1$ actually holds and output the result to the qubit, and then apply the gates additionally controlled on the qubit, if necessary. For small enough d , brute-force multi-controlled NOT gates would do the job without ruining efficiency.

3.4 Oracle O_H

When non-zero H_{xy} 's of the matrices (3.2) have simple dependence on a difference $(x - y)$, a naive way to implement the oracle computation $O_H |x, y\rangle |z\rangle = |x, y\rangle |z \oplus H_{xy}\rangle$ is to first read out $(x - y)$ and then bitwise-XOR the corresponding element H_{xy} . The former can be realized for example by adding x and $(-y - 1)$, and the latter can be realized by (hard-coded) bitwise NOT gates controlled on the difference, i.e. by placing NOT gates acting on qubits corresponding to *set-bits* of the number H_{xy} . The quantum circuit is as

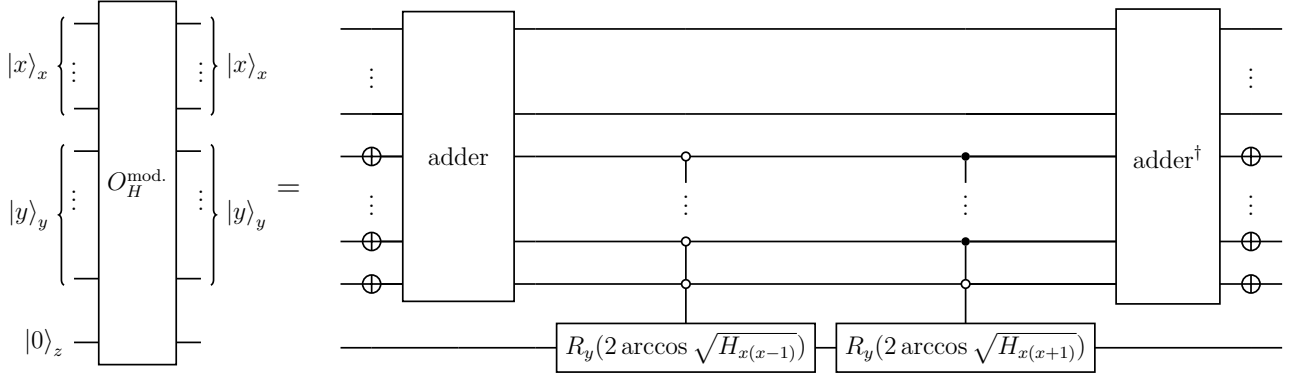


followed by suitable uncomputation, namely



again with n -qubit registers x, y and a register z with suitable size to store values.⁸ This time the circuit consumes $2 \times 2n + 2 \times 2(n-1) = 8n - 2$ Toffoli gates by a naive counting, as the multi-controlled gates are decomposed as in Appendix A.3 with $2(n-1)$ Toffoli gates.⁹

As already mentioned in Sec. 2, for actual usage, there is no need to first load the value of H_{xy} and then do the corresponding rotation; one can directly implement the rotations in-place. The quantum circuit of the modified oracle is given as



Another point worth mentioning here is about exceptional operations including those concerning “boundary conditions.” In Eq. (3.2), the condition for H_{xy} to be (possibly) non-zero involved taking modulo 2^n (due to the periodic boundary condition of the system), resulting in a *circulant* matrix. However, by inserting a bitwise-XOR (or corresponding rotation) gate controlled on the x register in addition to the y register between two adders in the above circuit, one can selectively *undo* the operation and kill unnecessary elements. For example, by acting controlled- $R_y(-2 \arccos \sqrt{H_{x(x-1)}})$ gate only when $x = 0$, one can in effect eliminate the $H_{0(n-1)}$ element. Doing the same thing for $H_{(n-1)0}$, one can realize an oracle O_H for a *tridiagonal* (or more generally a *band*) version of the original matrix (corresponding to a fixed boundary condition), without much cost.

⁸ For more generic band matrices, one can suitably add corresponding multi-controlled bitwise-XOR gates for $H_{x(x\pm 2)}$, $H_{x(x\pm 3)}$, and so on (where there is also a chance that, by sorting multi-controlled operations, adjacent ones can be contracted).

⁹ If the output of the first adder is guaranteed to be either $+1$ or -1 , one does not need to multi-control the $\oplus H_{xy}$ gate and a single-control operation is sufficient. This reduces the number of Toffoli gates used in the circuit and thus makes the computation faster (and alludes to the yet-more-efficient implementation presented in Appendix B), but here we stick to the naive implementation for ease of understanding.

3.5 Example 1: equal spring constants

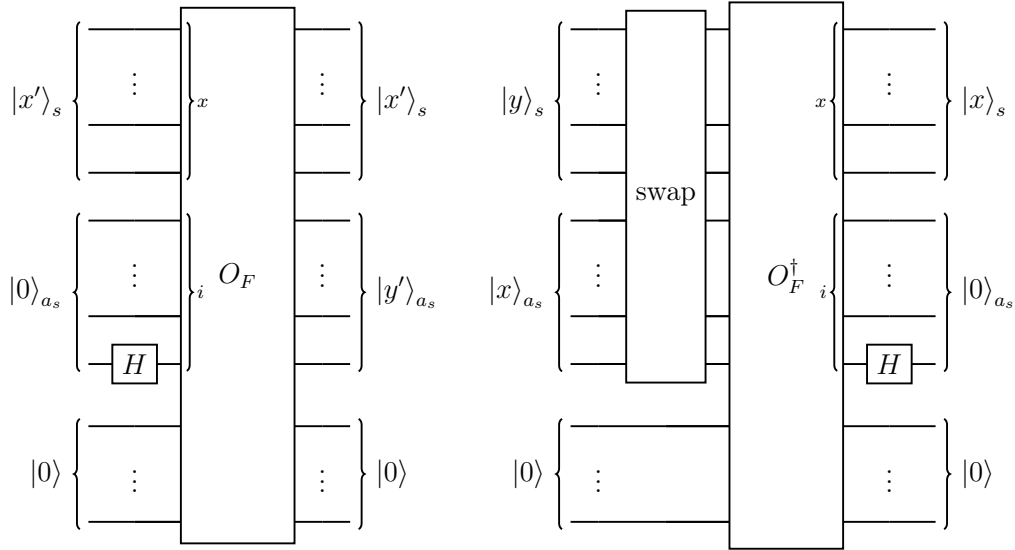
Now let us consider a simple system of $N = 2^n$ point masses of equal mass m connected by springs with equal spring constant k . The matrix (3.1) (up to a constant factor k/m) becomes

$$H_{xy}^{\text{original}} = \begin{cases} 1 & (|x - y| = 1) \\ -2 & (|x - y| = 0) \\ 0 & (\text{otherwise}) \end{cases} \quad (3.3)$$

and one can forget about the diagonal elements by considering $H = H^{\text{original}} + 2I$.¹⁰

Since all the non-zero matrix elements take the same value, things are extremely simplified; the controlled rotation parts of the algorithm become trivial, and therefore one can safely skip the steps involving ancillary qubits a_1 , a_2 , and v (and thus completely discard them), making the oracle O_H unnecessary as a result. This indeed makes sense because all we need is mere information about the position of non-zero matrix elements and not the values themselves.

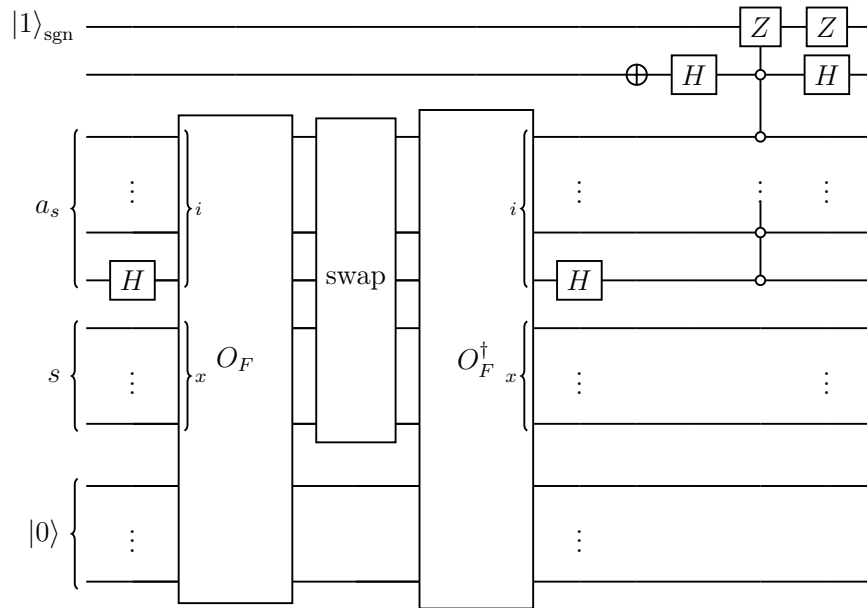
Anyway, following the description in Sec. 2.1, an explicit circuit for the unitary U_H is given by concatenating two circuit components corresponding to U_1 and U_2^\dagger



from which one can immediately obtain a circuit for the unitary U_H^* as described in Sec. 2.2.

¹⁰ The problem itself is just a special case of that considered in [CLVBY22, Sec. 4.2], but the emphasis is put on somewhat complementary aspects, so to speak.

An important point to note is that addition of control qubits to U_H is equivalent to that to the “swap” gate alone, since the net output of the circuit is the same even if the O_F - O_F^\dagger pair and the H - H pair are not controlled on the additional qubits.¹¹ Taking this trick into account, the unitary U_H^* is reduced to a $(4n + 2)$ -qubit circuit (including n ancillary qubits for multi-controlled gates (one of which is also used for adders) omitted in the diagram)



where the latter half of (controlled-) U_H and the former half of (controlled-) U_H^\dagger which do not involve control qubits are canceled out, and the two controlled-“swap”s are combined into a single (non-controlled) “swap.” As a result, a naive counting of Toffoli gates consumed by a controlled- U_H^* (to be fed into the QPE) as a whole (again keeping the trick in mind) is a sum of

- two O_F 's: $2 \times 4n$
- a controlled-“swap” (cf. Appendix A.4): n
- a multi-controlled gate at the end (cf. Appendix A.3): $2[(n + 2) - 1]$

which is equal to $11n + 2$.

¹¹ In fact, this is a special case of the trick mentioned in Appendix A.2.

3.6 Example 2: alternating spring constants

Let us next consider a slight generalization where one has alternating two spring constants k_1, k_2 . Without loss of generality, one can assume $k_1 < k_2$ and the equation of motion for the i -th point mass to be

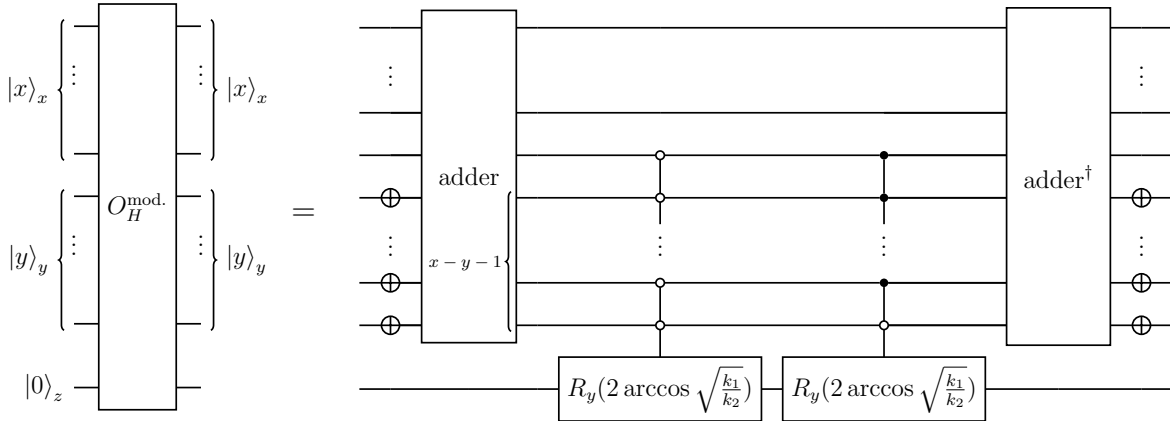
$$m\ddot{x}_i = \begin{cases} k_1(x_{i+1} - x_i) - k_2(x_i - x_{i-1}) & (i \text{ even}), \\ k_2(x_{i+1} - x_i) - k_1(x_i - x_{i-1}) & (i \text{ odd}). \end{cases}$$

The matrix (3.1) (up to a constant factor $\frac{1}{m}$) becomes¹²

$$H_{xy}^{\text{original}} = \begin{cases} k_1 & (\text{“}x \text{ even and } x - y = +1\text{” or “}x \text{ odd and } x - y = -1\text{”}) \\ -(k_1 + k_2) & (x - y = 0) \\ k_2 & (\text{“}x \text{ odd and } x - y = +1\text{” or “}x \text{ even and } x - y = -1\text{”}) \\ 0 & (\text{otherwise}) \end{cases} \quad (3.4)$$

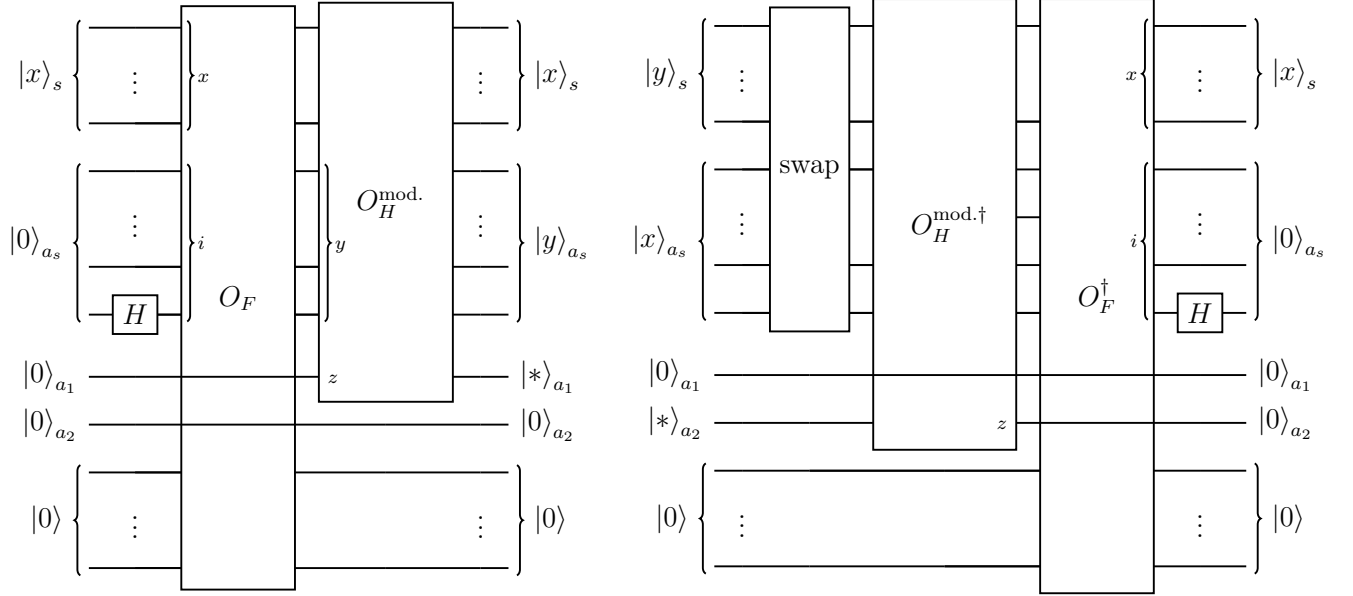
and one can consider $H = \frac{1}{k_2}[H^{\text{original}} + (k_1 + k_2)I]$ as a target matrix.

For this problem, we further modify the $O_H^{\text{mod.}}$ oracle; we add the topmost additional control qubit to the controlled rotation gates to identify the parity of x . Then, non-trivial rotations are carried out for $H_{xy} = \frac{k_1}{k_2}$ (while for $H_{xy} = \frac{k_2}{k_2} = 1$ rotations are trivial as $\arccos 1 = 0$ and thus unnecessary), which can be implemented as

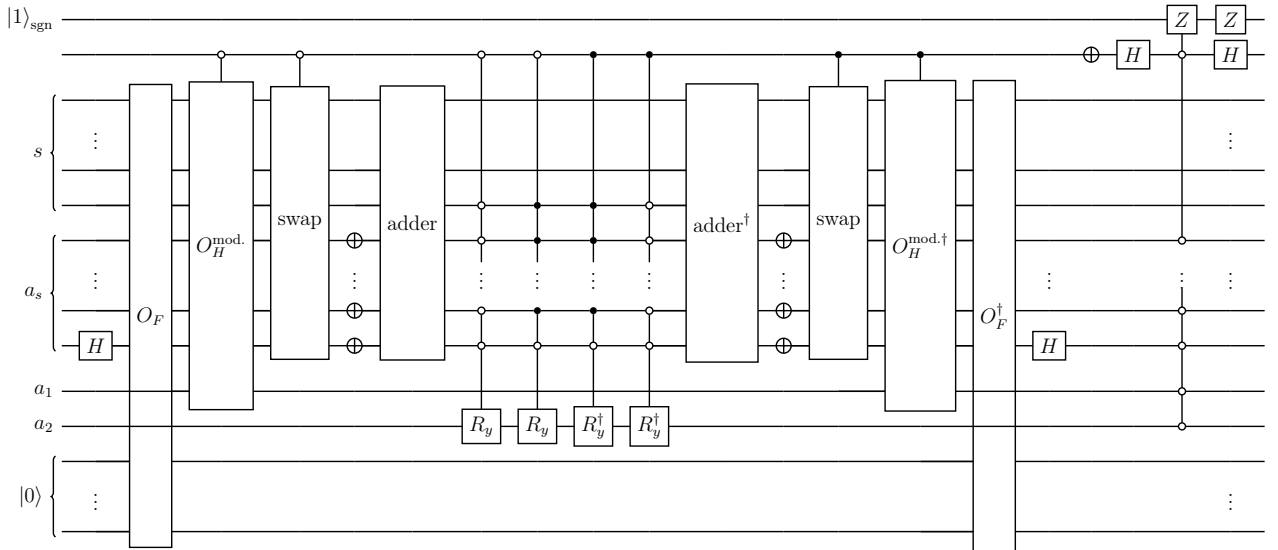


¹² This is actually equivalent to a Hamiltonian of the Su-Schrieffer-Heeger model [SSH79, SSH80], which describes a polyacetylene as a dimer chain consisting of alternating single (σ) and double (π) bonds, and suggests potential utility of non-LCU-based qubitization even in quantum chemistry/physics problems.

The circuit of the unitary U_H should be given by concatenating U_1 and U_2^\dagger as



As before, when adding control qubits to U_H , one does not need to add them to the O_F - O_F^\dagger pair, the H - H pair, and the adder-adder † pairs inside $O_H^{\text{mod.}}$'s. As a result, U_H^* is reduced to a $(4n + 6)$ -qubit circuit (including $(n + 2)$ ancillary qubits (suitably recycled) for the multi-controlled gates) as



Therefore, a naive counting of Toffoli gates consumed by a controlled- U_H^* is a sum of

- two O_F 's: $2 \times 4n$
- two multi-controlled- $O_H^{\text{mod.}}$'s: $2 \times \left[2 \times 2n + 2 \times 2\{(n+3) - 1\} \right]$
- two multi-controlled-“swap”s: $2 \times \left[n \times 2(3 - 1) \right]$
- two adders: $2 \times 2n$
- multi-controlled R_y 's (suitably permuted and paired up): $2 \times 2[(n+3) - 1]$
- a multi-controlled gate at the end: $2[(n+4) - 1]$

which is equal to $42n + 30$. The results are summarized as follows:

	$\#(\text{logical qubits})/U_H^*$	$\#(\text{Toffoli gates})/\text{controlled-}U_H^*$
Example 1	$4n + 2$	$11n + 2$
Example 2	$4n + 6$	$42n + 30$

Table 1: Summary of the costs necessary to solve the problems for 2^n point masses.

Note that the circuit implementations in this section are presented in a redundant form which (is easier to understand and) extends to more complicated problems at similar cost. As a result, they are far from optimal for the specific examples, and there is in fact plenty of room for *ad hoc* cost reduction by directly exploiting the structures of each problem. Although it is not our primary focus to reduce the costs as much as possible for the toy models, we present an example of fine-tuned implementation for Example 2 in Appendix B, which consumes far fewer qubits and Toffoli gates compared to the naive implementation.

3.7 Generalization: multiple layers

In passing, we also mention a more abstract level of oracle utilization. Consider a generic system of K point masses (not necessarily sparsely) connected to each other. Then, one can fabricate oracles $O_F^{\text{full}}, O_H^{\text{full}}$ for a system of $N = K \times L$ point masses comprised of L copies of the original system layered on top of each other, if oracles $O_F^{\text{sub}}, O_H^{\text{sub}}$ slightly modified as follows for the original system are available somehow: For a x -th point mass ($x \in \{1, \dots, K\}$) of a l -th layer ($l \in \{1, \dots, L\}$),

$$O_F^{\text{sub}} |x, i\rangle |0\rangle = |x, y_i\rangle |\Delta l_i\rangle$$

where i labels the spring connecting the x -th point mass to a y_i -th point mass of a $(l + \Delta l_i)$ -th layer, and

$$O_H^{\text{sub}} |x, y\rangle |\Delta l\rangle |z\rangle = |x, y\rangle |\Delta l\rangle |z \oplus H_{\Delta l, xy}\rangle$$

where $H_{\Delta l \neq 0, xy}$ describes connections between different layers. For example for the simplest case, Δl_i is either $-1, 0$, or $+1$, and the underlying matrices satisfy $H_{-1, xy} = -H_{+1, yx}$.

The target oracle O_F^{full} for the full system

$$O_F^{\text{full}} |x, i\rangle |l, 0\rangle = |x, y_i\rangle |l, l + \Delta l_i\rangle$$

can be realized by first applying O_F^{sub} and then applying an adder. Similarly, the oracle O_H^{full} for the full system

$$O_H^{\text{full}} |x, y\rangle |l, l + \Delta l\rangle |z\rangle = |x, y\rangle |l, l + \Delta l\rangle |z \oplus H_{\Delta l, xy}\rangle$$

can be realized just by applying O_H^{sub} . This allows us to analyze large systems with repetitive structure, which we expect to be in high demand for many practical applications. In particular, assuming that each layer is connected to a constant (i.e. L -independent) number of other layers (so that $H_{\Delta} \neq 0$ only for a limited number of Δl 's, which is often the case), this construction is exponentially efficient in terms of L , the number of repetitions, as dependence on it arises only from the adder of O_F^{full} . Also, note that the previous examples can be regarded as special instances of this generic construction where $(K, L) = (1, 2^n)$ or $(2, 2^{n-1})$ (instead of $(2^n, 1)$; original $|x, y\rangle$ corresponds to $|l, l + \Delta l\rangle$ from this point of view).

4 Initial states and their preparation

The remaining necessary ingredient to carry out a quantum phase estimation algorithm is an initial state upon which a sequence of powers-of-unitary is applied. If one can prepare an exact eigenstate $|\psi_{\text{exact}}\rangle$ of the unitary, then the phase estimation outputs the desired eigenvalue after a single iteration of the whole circuit. On the other hand, if one can only prepare an approximate eigenstate $|\psi_{\text{approx.}}\rangle$ of the unitary instead, then the success probability of QPE is given by the overlap $|\langle\psi_{\text{approx.}}|\psi_{\text{exact}}\rangle|^2$, meaning that the expectation value of the number of iterations necessary to extract a correct eigenvalue is its reciprocal. While it is almost impossible to prepare the ideal state $|\psi_{\text{exact}}\rangle$ in general, it is often assumed that some *nice* approximate state $|\psi_{\text{approx.}}\rangle$ can be efficiently prepared somehow, without ruining the exponential speedup over classical computation. In this section, we propose a naive way of state preparation for the problems of interest, and examine its effectiveness.

4.1 Proposal

Here we adopt an approximate eigenvector of the $2^n \times 2^n$ matrix H as the input state to a QPE algorithm, “approximating” the eigenstate (2.1) of the unitary U_H^* .¹³ One way to prepare it is the following: take small enough 2^m so that one can classically compute (within reasonable time) the exact eigenvector $|\psi_m\rangle$ of an “approximate H ” whose size is $2^m \times 2^m$. Encoding this state to m qubits by hand and then adding $(n - m)$ qubits set to $|+\rangle$, one can create an n -qubit state

$$|\psi_n^{(m)}\rangle := |\psi_m\rangle \otimes \frac{|00\dots 0\rangle + \dots + |11\dots 1\rangle}{\sqrt{2^{n-m}}}$$

which serves as an approximation to the eigenvector $|\psi_n\rangle$ of the target $2^n \times 2^n$ matrix H . For example, for $m = 2$ and $n = 4$, the procedure can be expressed as

$$\begin{aligned} |\psi_m\rangle = a|00\rangle + b|01\rangle + c|10\rangle + d|11\rangle \quad \mapsto \quad |\psi_n^{(m)}\rangle = & \frac{a}{2}(|0000\rangle + |0001\rangle + |0010\rangle + |0011\rangle) \\ & + \frac{b}{2}(|0100\rangle + |0101\rangle + |0110\rangle + |0111\rangle) \\ & + \frac{c}{2}(|1000\rangle + |1001\rangle + |1010\rangle + |1011\rangle) \\ & + \frac{d}{2}(|1100\rangle + |1101\rangle + |1110\rangle + |1111\rangle). \end{aligned}$$

The point of this method is that the desired approximate state can be prepared in an exponentially efficient manner in the sense that it only involves insertions of exponentially small number of qubits compared to the size (i.e. 2^n) of the state.

¹³ So the success probability of the QPE algorithm is about 0.5 (which is large enough for our purpose).

4.2 Numerical experiments

To check how well this method approximates the exact state, we compute and compare approximate eigenvectors $|\psi_n^{(m)}\rangle$ for relatively small 2^n . As a naive choice, here we just take the $2^m \times 2^m$ -matrix version of Eq. (3.2) as an “approximate H ”; for Example 1, the results are as follows:

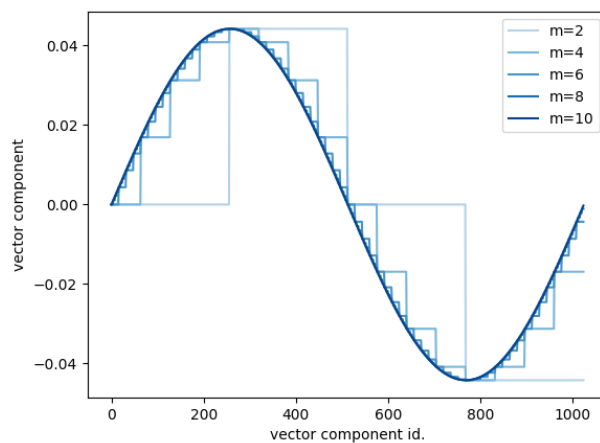


Figure 1: Approximate fundamental eigenvectors $|\psi_n^{(m)}\rangle$ of the matrices (3.3) of Example 1 for $n = 10$, rescaled and aligned.

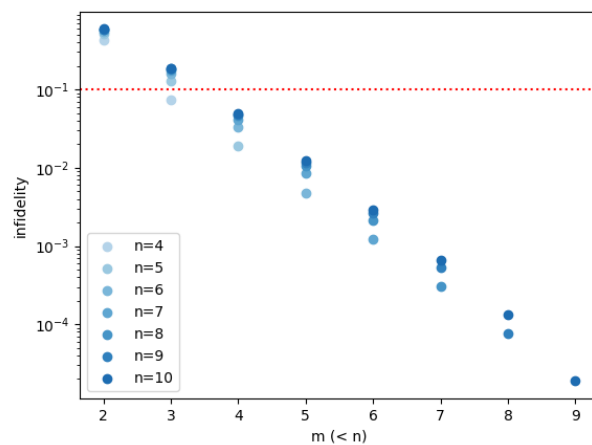
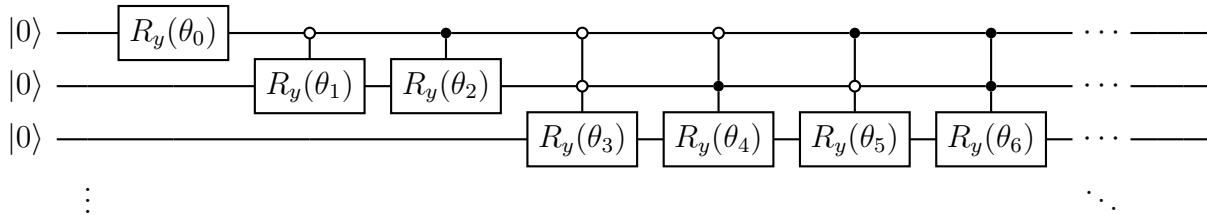


Figure 2: Infidelity $1 - |\langle \psi_n | \psi_n^{(m)} \rangle|^2$ between the exact fundamental eigenvectors $|\psi_n\rangle$ and approximate eigenvectors $|\psi_n^{(m)}\rangle$ of the matrices (3.3). The red dotted horizontal line denotes infidelity 0.1, implying that $m = 3$ is already a *good* approximation.

For Example 2, the results are basically the same, but one might want to consider the matrices (3.3) with $k = \frac{k_1+k_2}{2}$ instead in order to regard the approximation as *coarse graining*.

In either case, eigenvectors for very small 2^m already seem to approximate those for large 2^n quite well. In fact, the infidelity $1 - |\langle \psi_n | \psi_n^{(m)} \rangle|^2$ is about 0.1 for $m = 3$ for any $n (\leq 10)$, which is reasonably small and the corresponding *leaven* state $|\psi_m\rangle$ is easy to prepare. One naive way to do this is by $(2^m - 1)$ sequential (controlled) rotations as



where for $|\psi_m\rangle = \sum_{i=0}^{2^m-1} a_i |i\rangle$ ($a_i \in \mathbb{R}$) the angles $\{\theta_i\}$ are precomputed as

$$\begin{aligned} \theta_0 &= 2 \arccos \sqrt{\frac{a_0^2 + a_1^2 + \dots + a_{2^m-1}^2}{a_0^2 + a_1^2 + \dots + a_{2^m-1}^2 - 1}}, \\ \theta_1 &= 2 \arccos \sqrt{\frac{a_0^2 + a_1^2 + \dots + a_{2^{m-2}-1}^2}{a_0^2 + a_1^2 + \dots + a_{2^{m-1}-1}^2}}, \\ \theta_2 &= 2 \arccos \sqrt{\frac{a_{2^{m-1}}^2 + a_{2^{m-1}+1}^2 + \dots + a_{2^{m-1}+2^{m-2}-1}^2}{a_{2^{m-1}}^2 + a_{2^{m-1}+1}^2 + \dots + a_{2^m}^2 - 1}}, \end{aligned}$$

and so on, but one can also use more intricate circuits such as the PREPARE [BGB⁺18], at the expense of additional qubits and gates.

5 Resource estimation

In order to implement a quantum phase estimation algorithm on actual quantum devices, one has to employ quantum error-correcting codes and make the circuit fault-tolerant. One of the popular schemes used in previous resource estimation literature is the *surface code* [Kit97, BK98, DKLP01] based on the *lattice surgery* [HFDM11], as it achieves relatively high threshold error rates using only local interactions between nearest-neighbor qubits on an array, allowing it to possess high modularity.

The overhead due to this process is mainly twofold: encoding of logical qubits of the quantum circuit into physical qubits, and distillation of the *magic states* to be consumed to realize non-Clifford gates [BK04]. In this section, we examine them in order and give a very rough estimation¹⁴ of the number of necessary physical qubits and actual runtime, following [Lit18, Lit19]. Notations and details of parameters are summarized below.

parameter	description	assumed value
$\epsilon_{\text{prec.}}$	required precision of eigenvalues	10^{-4}
ϵ_{fail}	target failure rate of the whole circuit	10^{-2}
$p_{\text{phys.}}$	physical error rate of elementary operations	10^{-3}
t_{cycle}	code cycle time	$1 \mu\text{s}$

5.1 Encoding

Given an n_{logical} -qubit quantum circuit, one first needs to store the qubits in a larger *block* designed to enable them to consume magic states via lattice surgery. There is a trade-off between the block size $b(n_{\text{logical}})$ and the necessary code cycles c_{consume} for a magic state consumption, and the two extreme cases taken up in [Lit18] are the following:

block type	$b(n_{\text{logical}})$	c_{consume}
compact	$\lceil \frac{n_{\text{logical}}+2}{2} \rceil \times 3$	$9d_{\text{code}}$
fast	$\min_{1 \leq k \leq n_{\text{logical}}} (2k + 1) \cdot (\lceil \frac{n_{\text{logical}}}{k} \rceil + 1)$	d_{code}

¹⁴ Precise estimation involves innumerable subtleties (e.g. execution of Clifford gates, routing of qubits), and here we turn a blind eye to them and content ourselves with a superficial analysis. The results are hopefully within an order of magnitude of the true values.

where d_{code} is the code distance. Then, each of the $b(n_{\text{logical}})$ logical qubits is converted to d_{code}^2 physical qubits, equipped with another d_{code}^2 physical qubits used for syndrome measurements. Since the logical error rate per logical qubit per code cycle (round) is known [FWH10, Fig. 8] to be approximated as

$$p_{\text{logical}} = 0.1 \cdot (100 p_{\text{phys.}})^{\lceil \frac{d_{\text{code}}}{2} \rceil},$$

the code distance d_{code} to be adopted is determined by requiring

$$p_{\text{logical}} \cdot b(n_{\text{logical}}) \cdot \max(c_{\text{consume}}, c_{\text{produce}}) \cdot n_T < \epsilon_{\text{fail}} \quad (5.1)$$

where c_{produce} is the (net) necessary code cycles for production of a (distilled) magic state at *factories* built out of n_{distill} physical qubits in total, and n_T is the number of T gates in the quantum circuit (after suitably decomposing all the non-Clifford gates). Making a choice of d_{code} satisfying Eq. (5.1), one can calculate the total number of necessary physical qubits and actual runtime as

$$\begin{aligned} n_{\text{phys.}} &= b(n_{\text{logical}}) \cdot 2d_{\text{code}}^2 + n_{\text{distill}}, \\ t_{\text{total}} &= \max(c_{\text{consume}}, c_{\text{produce}}) \cdot n_T \cdot t_{\text{cycle}}. \end{aligned}$$

For the analysis below however, we will focus on Toffoli gates instead of T gates and correspondingly the factor $\max(c_{\text{consume}}, c_{\text{produce}}) \cdot n_T$ is suitably replaced.

5.2 Realization of Toffoli gates

One way to execute a Toffoli gate is by consuming a Toffoli or CCZ state which can be synthesized from magic states [Eas12, Jon12, CH16a, CH16b]. According to [Lit19], one can construct a *factory* consisting of 0.5×10^5 physical qubits, which can ship a CCZ state with small enough infidelity ($< 10^{-10}$) every 60 code cycles. As one typically has $d_{\text{code}} \geq 7$ (and thus $9d_{\text{code}} > 60$), we adopt the *fast block* above for encoding and operate n_{factory} factories so that

$$\begin{aligned} n_{\text{distill}} &= 0.5 \times 10^5 \cdot n_{\text{factory}}, \\ \max(c_{\text{consume}}, c_{\text{produce}}) &= \max(d_{\text{code}}, \frac{60}{n_{\text{factory}}}). \end{aligned}$$

5.3 Case study

Let us take up the naive implementations of examples in Sec. 3, expecting that required costs are not that different from those of slightly more general problems and thus give indications thereof. The quantum circuit to start with is that of quantum phase estimation with unitary U_H^* described in Sec. 3.5 or Sec. 3.6 plugged in, where for the latter one has

$$\begin{aligned} n_{\text{logical}} &= (4n + 6) + \left\lceil \log_2 \frac{1}{\epsilon_{\text{prec.}}} \right\rceil, \\ n_{\text{Toffoli}} &= (42n + 30) \times (2^{\lceil \log_2 \frac{1}{\epsilon_{\text{prec.}}} \rceil} - 1). \end{aligned}$$

If one takes $\epsilon_{\text{prec.}} = 10^{-4}$ (and ignores the normalization of H for simplicity), it turns out that $n_{\text{Toffoli}} \lesssim 10^8$ for $n \lesssim 128$, and thus the CCZ state above with infidelity $< 10^{-10}$ is reasonable to use.¹⁵ Following the preceding argument, some rough estimates are given as follows:

order of matrix	d_{code}	# of logical/physical qubits	# of Toffoli gates	runtime
2^{32}	23	330 / $\sim 4.5 \times 10^5$	$\sim 0.6 \times 10^7$	~ 6 min.
2^{64}	25	594 / $\sim 8.4 \times 10^5$	$\sim 1.2 \times 10^7$	~ 12 min.
2^{128}	25	1128 / $\sim 15.1 \times 10^5$	$\sim 2.3 \times 10^7$	~ 24 min.
order of matrix	d_{code}	# of logical/physical qubits	# of Toffoli gates	runtime
2^{32}	25	336 / $\sim 5.2 \times 10^5$	$\sim 2.3 \times 10^7$	~ 23 min.
2^{64}	25	608 / $\sim 8.6 \times 10^5$	$\sim 4.5 \times 10^7$	~ 45 min.
2^{128}	27	1134 / $\sim 17.5 \times 10^5$	$\sim 8.9 \times 10^7$	~ 90 min.

Table 2: Summary of very rough estimates of the costs necessary to solve the problems of Example 1 (above) and 2 (below) for 2^n point masses, $\epsilon_{\text{prec.}} = 10^{-4}$, $t_{\text{cycle}} = 1 \mu\text{s}$ (and $k_2 = \frac{1}{2}$ for the latter), using the fast block of [Lit18] and $n_{\text{factory}} = 2$ factories of [Lit19] mentioned in the previous subsections. To estimate the runtime, we also assumed that the QPE is run twice (since the success probability was about 0.5 as mentioned in Sec. 4).

¹⁵ Here we also ignore the costs required for (not only Clifford gates but also) Pauli rotation gates in both the unitary U_H^* and the inverse Quantum Fourier Transform component, whose numbers are independent of the matrix order 2^n . They can be fault-tolerantly implemented by decomposition into Clifford+ T gates, combining the methods of [RS14] and [KMM12], which roughly uses $3 \log_2 \frac{1}{\epsilon_{\text{prec.}}} \cdot [4 \cdot \frac{1}{\epsilon_{\text{prec.}}} + \frac{1}{2} (\log_2 \frac{1}{\epsilon_{\text{prec.}}})^2] \sim 10^6 T$ gates and should be negligible compared to the Toffoli gates' cost for large 2^n .

We again stress that they are given only as a demonstration with many finer points swept under the rug, and the precise values themselves have no actual meaning at all.¹⁶ The interested reader is referred to e.g. [GF19, LBG⁺20] and references therein for more refined analyses using CCZ state factories.

Acknowledgments

The authors would like to thank Yuya O. Nakagawa and Shoichiro Tsutsui for careful reading of and comments on the draft. The authors are also deeply grateful to Christoph Sünderhauf for kindly pointing out that the method of [SCC23] can be applied to our toy problems and sharing an explicit circuit construction with far fewer qubits and Toffoli gates (and even smaller subnormalization) based on it, which inspired a further-improved implementation by the authors presented in Appendix B.

¹⁶ Also, if one *really* wants to do the computation for this specific problem, it would be better to use a more efficient circuit, for example the one described in Appendix B, while the cost of the rotation gates might not be negligible even for $n = 128$.

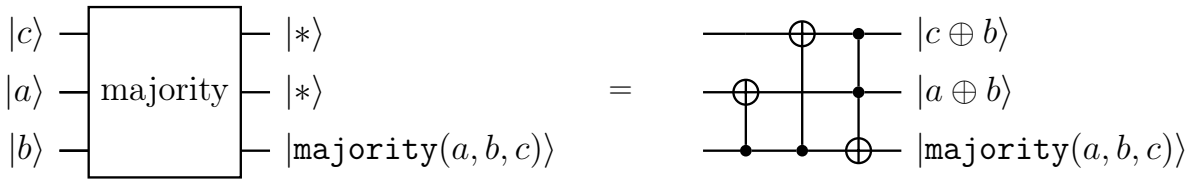
A Quantum arithmetic and related operations

We summarize the necessary modules to decompose a full circuit into elementary gates.

A.1 Adder

It is known that a sum (modulo 2^n) of two n -bit integers encoded in quantum states can be computed using only a single ancillary qubit [CDKM04]. The basic strategy is to first compute all the *carries*, and then do the summation. Correspondingly, the adder consists of two elementary components.

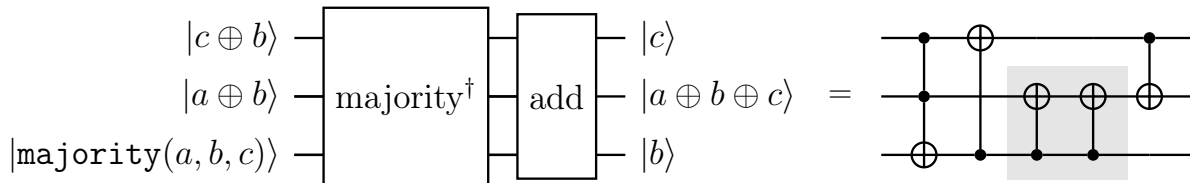
The first component is a *majority* gate, implemented as



where $a, b \in \{0, 1\}$ correspond to summand bits and $c \in \{0, 1\}$ corresponds to a carry from lower bits. The purpose of the gate is to output a carry of the addition $c + a + b$, which is equal to $\text{majority}(a, b, c)$.

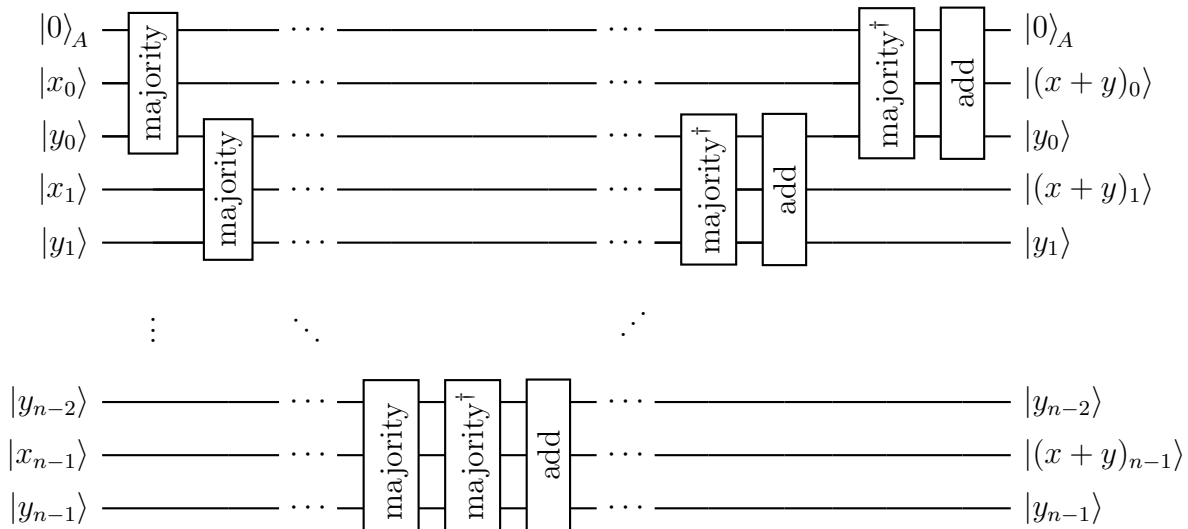
If $b = 0$, one does not have to do anything to the corresponding qubit $|b\rangle$, except when $\text{majority}(a, b, c) = 1$, i.e. when both c and a are 1, which can be realized by a flipping of b conditioned on $c = a = 1$. This explains the rightmost Toffoli gate. On the other hand, if $b = 1$, one has to flip this bit when $\text{majority}(a, b, c) = 0$ i.e. when both c and a are 0, and one can utilize the same Toffoli gate with two preceding CNOT gates to achieve this.

The second component is an *un-majority + add* gate, implemented as



which (undoes the *majority* operation and then) outputs the bitwise summation result $a \oplus b \oplus c$. Here, the two CNOT gates in the shaded box cancel out.

With these two components, the desired adder of two n -bit integers x, y is realized using only a single ancillary qubit A as



where the top qubit of each majority gate always encodes a carry and the other two qubits encode summands. Here, a naive counting tells us that the number of necessary Toffoli gates for each full adder of n -bit integers is $2n$.¹⁷

Also, note that a controlled adder can be realized using $4n$ Toffoli gates, thanks to the trick mentioned in Appendix A.2; one just needs to control the first CNOT gates of majority gates and the last CNOT gates of un-majority + add gates, as the remaining gates are in pairs and need not be controlled.

¹⁷ The number of gates can be *halved* (although the count is in terms of T gates) at the cost of additional n ancillary qubits (and their measurements) [Gid17], but for the sake of simplicity we will stick to the naive adder explained above.

A.2 Controlled unitaries

When adding control qubits to a large quantum gate which consists of multiple (smaller) gates, there is a useful trick to keep in mind; if there exists a subsequence of gates which as a whole constitutes a trivial gate, one does not have to add control qubits to those gates as the overall action does not change.

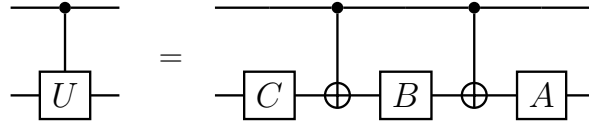
An especially important example is the following: As is well-known (see e.g. a standard textbook [NC00]), using three unitaries

$$\begin{aligned} A &= R_z(\beta) R_y\left(\frac{\gamma}{2}\right), \\ B &= R_y\left(-\frac{\gamma}{2}\right) R_z\left(-\frac{\beta+\delta}{2}\right), \\ C &= R_z\left(-\frac{\beta-\delta}{2}\right), \end{aligned}$$

one can construct an arbitrary single-qubit unitary (up to phase) as

$$U = AXBXC = \begin{pmatrix} e^{-i\frac{\beta+\delta}{2}} \cos \frac{\gamma}{2} & -e^{-i\frac{\beta-\delta}{2}} \sin \frac{\gamma}{2} \\ e^{+i\frac{\beta-\delta}{2}} \sin \frac{\gamma}{2} & e^{+i\frac{\beta+\delta}{2}} \cos \frac{\gamma}{2} \end{pmatrix}.$$

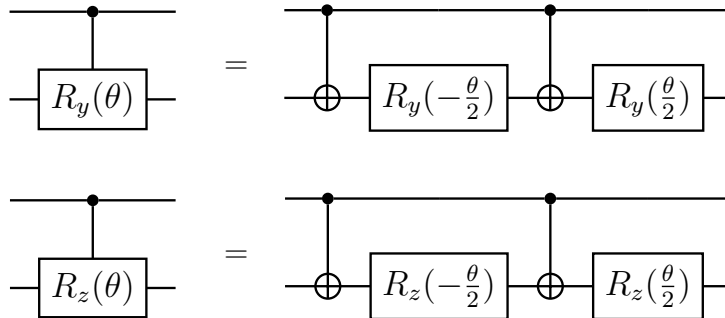
Given this form of decomposition, a controlled- U gate can be constructed as



by adding control qubits only to X gates, since $ABC = I$. Of particular interests are the following controlled-rotations:

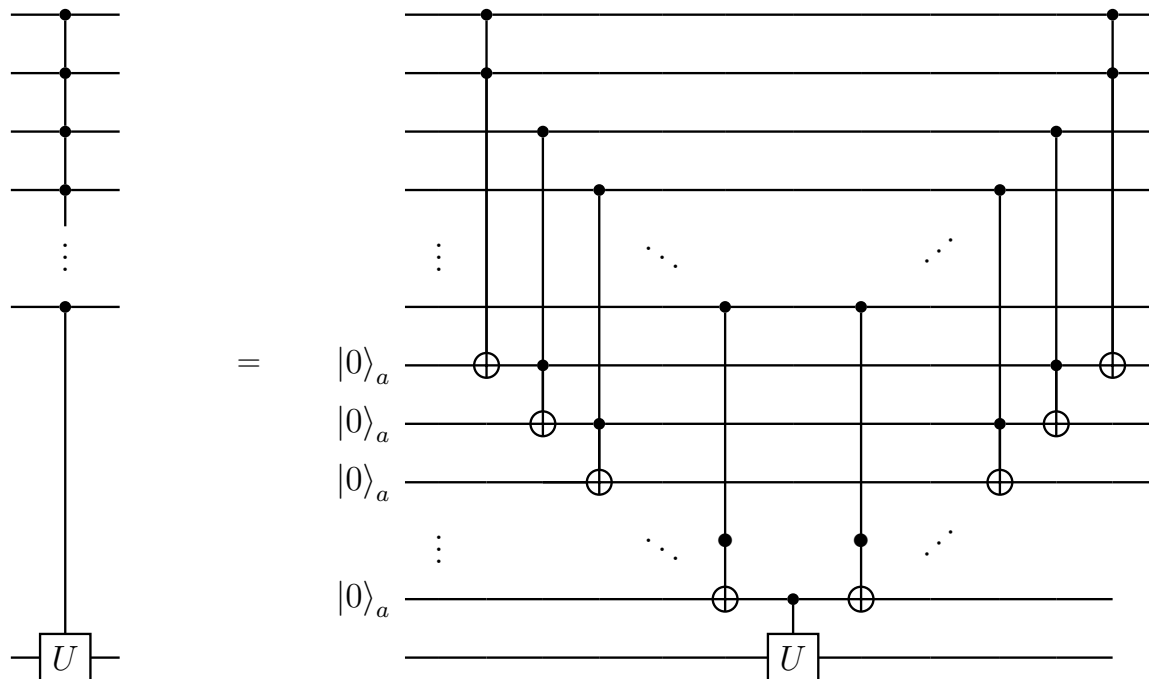
U	β	γ	δ
$R_y(\theta)$	0	θ	0
$R_z(\theta)$	x	0	$\theta - x$

where one can take $x = \frac{\theta}{2}$ for convenience.



A.3 Multi-controlled unitaries

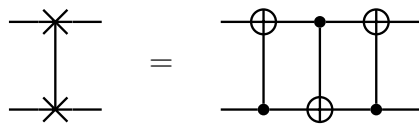
A multi-controlled gate can be immediately decomposed into a single-controlled gate sandwiched by cascaded Toffoli gates:



In other words, a unitary gate with n control qubits can be implemented at the cost of $2(n - 1)$ Toffoli gates and $(n - 1)$ ancillary qubits.

A.4 SWAP

A SWAP gate is also easy to decompose; it consists of three CNOT gates:



The first two CNOT gates swap the two qubits if the initial values are $(0, 1)$, while the last two CNOT gates swap the two qubits if the initial values are $(1, 0)$. Using the trick mentioned in Appendix A.2, a (multi-)controlled SWAP gate is realized by adding corresponding control qubits only to the middle CNOT gate.

B Speedrun

Here we give a fine-tuned circuit implementation of Example 2, which requires far fewer qubits and Toffoli gates compared to the naive one in Sec. 3.6. It is inspired by a construction à la [SCC23] provided by Christoph Sünderhauf, and essentially relies on a direct use of the index indicating the non-zero elements, without explicitly turning to the full row/column indices by the oracle O_F of Sec. 3.3.

If one can construct a unitary U_2 such that

$$U_2 |x\rangle_x |0\rangle_{a_1} |0\rangle_{a_2} = \begin{cases} \frac{1}{\sqrt{2}} \left[|x-1\rangle_s |0\rangle_{a_1} \left(\frac{k_1}{k_2} |0\rangle + \sqrt{1 - \left(\frac{k_1}{k_2}\right)^2} |1\rangle \right)_{a_2} + |x+1\rangle_s |1\rangle_{a_1} |0\rangle_{a_2} \right] & (x \text{ even}) \\ \frac{1}{\sqrt{2}} \left[|x+1\rangle_s |0\rangle_{a_1} \left(\frac{k_1}{k_2} |0\rangle + \sqrt{1 - \left(\frac{k_1}{k_2}\right)^2} |1\rangle \right)_{a_2} + |x-1\rangle_s |1\rangle_{a_1} |0\rangle_{a_2} \right] & (x \text{ odd}) \end{cases}$$

then taking U_1 to be an Hadamard gate acting on the ancilla qubit a_1

$$U_1 |y\rangle_s |0\rangle_{a_1} |0\rangle_{a_2} = |y\rangle_s \frac{|0\rangle_{a_1} + |1\rangle_{a_1}}{\sqrt{2}} |0\rangle_{a_2},$$

the product $U_2^\dagger U_1$ block-encodes the original matrix H (3.4) as

$$\langle x|_s \langle 0|_{a_1} \langle 0|_{a_2} U_2^\dagger U_1 |y\rangle_s |0\rangle_{a_1} |0\rangle_{a_2} \sim \begin{cases} \frac{k_1}{k_2} / 1 & (“x \text{ even}, x - y = +1 / -1”), \\ 1 / \frac{k_1}{k_2} & (“x \text{ odd}, x - y = +1 / -1”), \\ 0 & (\text{otherwise}). \end{cases}$$

Starting from a state $|x\rangle_s |0\rangle_{a_1} |0\rangle_{a_2}$, one can see that U_2 can be realized for example by sequentially acting

1. an Hadamard gate acting on a_1 ,

$$\text{making an equal-superposition state } \frac{1}{\sqrt{2}} \left(|x\rangle_s |0\rangle_{a_1} |0\rangle_{a_2} + |x\rangle_s |1\rangle_{a_1} |0\rangle_{a_2} \right),$$

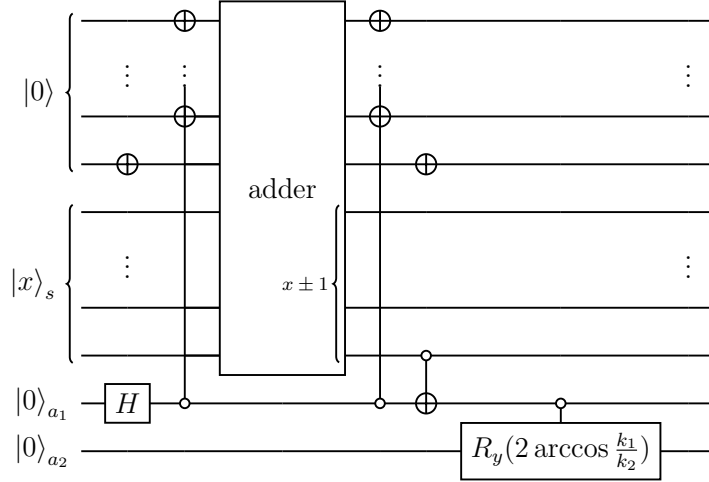
2. an adder with suitable preprocessing and uncomputation,

$$\text{turning the state into } \frac{1}{\sqrt{2}} \left(|x-1\rangle_s |0\rangle_{a_1} |0\rangle_{a_2} + |x+1\rangle_s |1\rangle_{a_1} |0\rangle_{a_2} \right),$$

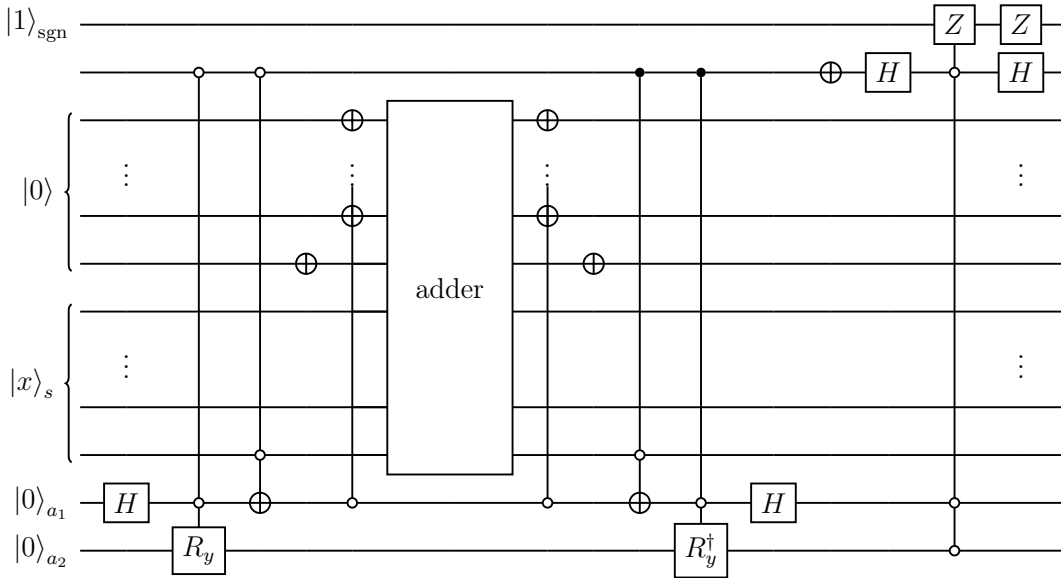
3. a CNOT gate controlled on the parity of x (i.e. the least significant (qu)bit of s) and targeting on a_1 , leading to

$$\begin{cases} \frac{1}{\sqrt{2}} \left(|x-1\rangle_s |0\rangle_{a_1} |0\rangle_{a_2} + |x+1\rangle_s |1\rangle_{a_1} |0\rangle_{a_2} \right) & (x \text{ even}) \\ \frac{1}{\sqrt{2}} \left(|x+1\rangle_s |0\rangle_{a_1} |0\rangle_{a_2} + |x-1\rangle_s |1\rangle_{a_1} |0\rangle_{a_2} \right) & (x \text{ odd}) \end{cases}$$

4. a controlled rotation controlled on a_1 and targeting on a_2 , achieving the desired state.



Again, addition of control qubits to $U_2^\dagger U_1$ does not require the Hadamard gates, the X gates, and the multiple CNOT gates to be controlled. As a result, the block encoding unitary $U_2^\dagger U_1$ can be qubitized into a $(2n + 6)$ -qubit circuit U_H^* (including two ancillary qubits for the multi-controlled gate and also for the adder) as



where the latter half of (controlled-) $U_2^\dagger U_1$ and the former half of (controlled-) $U_1^\dagger U_2$ which do not involve control qubits are canceled out, and the two controlled-adders are combined into a single (non-controlled) adder. Recalling that a controlled adder uses $4n$ Toffoli gates and controlling the CNOT gates following Appendix A.3 (instead of turning each into a Toffoli gate), a controlled- U_H^* can be realized using only $(4n + 24)$ Toffoli gates.

order of matrix	d_{code}	# of logical/physical qubits	# of Toffoli gates	runtime
2^{32}	23	198 / $\sim 3.1 \times 10^5$	$\sim 2.5 \times 10^6$	~ 3 min.
2^{64}	23	336 / $\sim 4.6 \times 10^5$	$\sim 4.6 \times 10^6$	~ 5 min.
2^{128}	25	608 / $\sim 8.6 \times 10^5$	$\sim 8.8 \times 10^7$	~ 9 min.

Table 3: Summary of very rough estimates of the costs necessary to solve the problems of Example 2 using the above fine-tuned circuit with the same settings as in Sec. 5.

Fortunately, this seemingly-drastic shortcut still retains flexibility to carry out additional exceptional operations described in Sec. 3.4. For example, rotation gates controlled not only on the a_1 register but also on the s register enables modifying each non-zero element, while expanding the a_1 register allows (at least conceptually) straightforward generalization of the construction to denser matrices, where the amount of necessary resources approach to those of the naive implementation as the matrix becomes denser and denser.

References

- [Ans] Ansys Innovation Courses, *Modal Analysis*, <https://courses.ansys.com/index.php/courses/modal-analysis/>.
- [BBK⁺23] R. Babbush, D. W. Berry, R. Kothari, R. D. Somma, and N. Wiebe, *Exponential quantum speedup in simulating coupled classical oscillators*, [arXiv:2303.13012 \[quant-ph\]](#).
- [BC09] D. W. Berry and A. M. Childs, *Black-box hamiltonian simulation and unitary implementation*, *Quantum Info. Comput.* **12** (2012) 29–62, [arXiv:0910.4157 \[quant-ph\]](#).
- [BCC⁺22] N. S. Blunt, J. Camps, O. Crawford, R. Izsák, S. Leontica, A. Mirani, A. E. Moylett, S. A. Scivier, C. Sünderhauf, P. Schopf, J. M. Taylor, and N. Holzmann, *Perspective on the current state-of-the-art of quantum computing for drug discovery applications*, *Journal of Chemical Theory and Computation* **18** (2022) 7001–7023, [arXiv:2206.00551 \[quant-ph\]](#).
- [BGB⁺18] R. Babbush, C. M. Gidney, D. W. Berry, N. Wiebe, J. McClean, A. Paler, A. Fowler, and H. Neven, *Encoding electronic spectra in quantum circuits with linear T complexity*, *Physical Review X* **8** (2018) 041015, [arXiv:1805.03662 \[quant-ph\]](#).
- [BGM⁺19] D. W. Berry, C. M. Gidney, M. Motta, J. R. McClean, and R. Babbush, *Qubitization of arbitrary basis quantum chemistry leveraging sparsity and low rank factorization*, *Quantum* **3** (2019) 208, [arXiv:1902.02134 \[quant-ph\]](#).
- [BK98] S. B. Bravyi and A. Y. Kitaev, *Quantum codes on a lattice with boundary*, [arXiv:quant-ph/9811052](#).
- [BK04] ———, *Universal quantum computation with ideal Clifford gates and noisy ancillas*, *Phys. Rev. A* **71** (2005) 022316, [arXiv:quant-ph/0403025](#).
- [BMT⁺22] M. E. Beverland, P. Murali, M. Troyer, K. M. Svore, T. Hoeffler, V. Kliuchnikov, G. H. Low, M. Soeken, A. Sundaram, and A. Vaschillo, *Assessing requirements to scale to practical quantum advantage*, [arXiv:2211.07629 \[quant-ph\]](#).

- [CDKM04] S. A. Cuccaro, T. G. Draper, S. A. Kutin, and D. P. Moulton, *A new quantum ripple-carry addition circuit*, [arXiv:quant-ph/0410184](#).
- [CEMM97] R. Cleve, A. Ekert, C. Macchiavello, and M. Mosca, *Quantum algorithms revisited*, *Proceedings of the Royal Society of London. Series A: Mathematical, Physical and Engineering Sciences* **454** (1998) 339–354, [arXiv:quant-ph/9708016](#).
- [CH16a] E. T. Campbell and M. Howard, *Unified framework for magic state distillation and multiqubit gate synthesis with reduced resource cost*, *Phys. Rev. A* **95** (2017) 022316, [arXiv:1606.01904 \[quant-ph\]](#).
- [CH16b] ———, *Unifying gate synthesis and magic state distillation*, *Phys. Rev. Lett.* **118** (2017) 060501, [arXiv:1606.01906 \[quant-ph\]](#).
- [CLVBY22] D. Camps, L. Lin, R. Van Beeumen, and C. Yang, *Explicit quantum circuits for block encodings of certain sparse matrices*, [arXiv:2203.10236 \[quant-ph\]](#).
- [DCdR⁺22] A. Delgado, P. A. M. Casares, R. dos Reis, M. S. Zini, R. Campos, N. Cruz-Hernández, A.-C. Voigt, A. Lowe, S. Jahangiri, M. A. Martin-Delgado, J. E. Mueller, and J. M. Arrazola, *Simulating key properties of lithium-ion batteries with a fault-tolerant quantum computer*, *Phys. Rev. A* **106** (2022) 032428, [arXiv:2204.11890 \[quant-ph\]](#).
- [DKLP01] E. Dennis, A. Kitaev, A. Landahl, and J. Preskill, *Topological quantum memory*, *J. Math. Phys.* **43** (2002) 4452–4505, [arXiv:quant-ph/0110143](#).
- [Eas12] B. Eastin, *Distilling one-qubit magic states into Toffoli states*, *Phys. Rev. A* **87** (2013) 032321, [arXiv:1212.4872 \[quant-ph\]](#).
- [FWH10] A. G. Fowler, D. S. Wang, and L. C. L. Hollenberg, *Surface code quantum error correction incorporating accurate error propagation*, *Quantum Info. Comput.* **11** (2011) 8–18, [arXiv:1004.0255 \[quant-ph\]](#).
- [GF19] C. Gidney and A. G. Fowler, *Flexible layout of surface code computations using AutoCCZ states*, [arXiv:1905.08916 \[quant-ph\]](#).
- [Gid17] C. Gidney, *Halving the cost of quantum addition*, *Quantum* **2** (2018) 74, [arXiv:1709.06648 \[quant-ph\]](#).

- [GSLW18] A. Gilyén, Y. Su, G. H. Low, and N. Wiebe, *Quantum Singular Value Transformation and beyond: Exponential improvements for quantum matrix arithmetics*, *STOC 2019: Proceedings of the 51st Annual ACM SIGACT Symposium on Theory of Computing (2019)* 193–204, [arXiv:1806.01838 \[quant-ph\]](#).
- [GWL⁺22] J. J. Goings, A. White, J. Lee, C. S. Tautermann, M. Degroote, C. Gidney, T. Shiozaki, R. Babbush, and N. C. Rubin, *Reliably assessing the electronic structure of cytochrome P450 on today’s classical computers and tomorrow’s quantum computers*, *Proceedings of the National Academy of Sciences* **119** (2022), [arXiv:2202.01244 \[quant-ph\]](#).
- [HFDM11] C. Horsman, A. G. Fowler, S. Devitt, and R. V. Meter, *Surface code quantum computing by lattice surgery*, *New Journal of Physics* **14** (2012) 123011, [arXiv:1111.4022 \[quant-ph\]](#).
- [ISH⁺22] A. V. Ivanov, C. Sünderhauf, N. Holzmann, T. Ellaby, R. N. Kerber, G. Jones, and J. Camps, *Quantum computation for periodic solids in second quantization*, *Phys. Rev. Res.* **5** (2023) 013200, [arXiv:2210.02403 \[quant-ph\]](#).
- [Jon12] C. Jones, *Low-overhead constructions for the fault-tolerant Toffoli gate*, *Phys. Rev. A* **87** (2013) 022328, [arXiv:1212.5069 \[quant-ph\]](#).
- [Kit95] A. Y. Kitaev, *Quantum measurements and the abelian stabilizer problem*, [arXiv:quant-ph/9511026](#).
- [Kit97] ———, *Fault tolerant quantum computation by anyons*, *Annals Phys.* **303** (2003) 2–30, [arXiv:quant-ph/9707021](#).
- [KLP⁺21] I. H. Kim, Y.-H. Liu, S. Pallister, W. Pol, S. Roberts, and E. Lee, *Fault-tolerant resource estimate for quantum chemical simulations: Case study on Li-ion battery electrolyte molecules*, *Phys. Rev. Res.* **4** (2022) 023019, [arXiv:2104.10653 \[quant-ph\]](#).
- [KMM12] V. Kliuchnikov, D. Maslov, and M. Mosca, *Fast and efficient exact synthesis of single-qubit unitaries generated by Clifford and T gates*, [arXiv:1206.5236 \[quant-ph\]](#).
- [LBG⁺20] J. Lee, D. W. Berry, C. Gidney, W. J. Huggins, J. R. McClean, N. Wiebe, and R. Babbush, *Even more efficient quantum computations of chemistry through*

- tensor hypercontraction*, *PRX Quantum* **2** (2021) 030305, [arXiv:2011.03494 \[quant-ph\]](#).
- [LC16] G. H. Low and I. L. Chuang, *Hamiltonian Simulation by Qubitization*, *Quantum* **3** (2019) 163, [arXiv:1610.06546 \[quant-ph\]](#).
- [Lit18] D. Litinski, *A Game of Surface Codes: Large-Scale Quantum Computing with Lattice Surgery*, *Quantum* **3** (2019) 128, [arXiv:1808.02892 \[quant-ph\]](#).
- [Lit19] ———, *Magic State Distillation: Not as Costly as You Think*, *Quantum* **3** (2019) 205, [arXiv:1905.06903 \[quant-ph\]](#).
- [NC00] M. A. Nielsen and I. L. Chuang, *Quantum computation and quantum information*, Cambridge University Press, 2000.
- [RBM⁺23] N. C. Rubin, D. W. Berry, F. D. Malone, A. F. White, T. Khattar, A. E. DePrince III, S. Sicolo, M. Kühn, M. Kaicher, J. Lee, and R. Babbush, *Fault-tolerant quantum simulation of materials using Bloch orbitals*, [arXiv:2302.05531 \[quant-ph\]](#).
- [RS14] N. J. Ross and P. Selinger, *Optimal ancilla-free Clifford+T approximation of z-rotations*, *Quantum Info. Comput.* **16** (2016) 901–953, [arXiv:1403.2975 \[quant-ph\]](#).
- [RWS⁺16] M. Reiher, N. Wiebe, K. M. Svore, D. Wecker, and M. Troyer, *Elucidating reaction mechanisms on quantum computers*, *Proceedings of the National Academy of Sciences* **114** (2017) 7555–7560, [arXiv:1605.03590 \[quant-ph\]](#).
- [SBW⁺21] Y. Su, D. W. Berry, N. Wiebe, N. Rubin, and R. Babbush, *Fault-tolerant quantum simulations of chemistry in first quantization*, *PRX Quantum* **2** (2021) 040332, [arXiv:2105.12767 \[quant-ph\]](#).
- [SCC23] C. Sünderhauf, E. Campbell, and J. Camps, *Block-encoding structured matrices for data input in quantum computing*, [arXiv:2302.10949 \[quant-ph\]](#).
- [SSH79] W. P. Su, J. R. Schrieffer, and A. J. Heeger, *Solitons in polyacetylene*, *Phys. Rev. Lett.* **42** (1979) 1698–1701.
- [SSH80] ———, *Soliton excitations in polyacetylene*, *Phys. Rev. B* **22** (1980) 2099–2111.

- [vBLH⁺20] V. von Burg, G. H. Low, T. Häner, D. S. Steiger, M. Reiher, M. Roetteler, and M. Troyer, *Quantum computing enhanced computational catalysis*, *Phys. Rev. Res.* **3** (2021) 033055, [arXiv:2007.14460](#) [quant-ph].
- [YOS⁺22] N. Yoshioka, T. Okubo, Y. Suzuki, Y. Koizumi, and W. Mizukami, *Hunting for quantum-classical crossover in condensed matter problems*, [arXiv:2210.14109](#) [quant-ph].
- [ZDdR⁺23] M. S. Zini, A. Delgado, R. dos Reis, P. A. M. Casares, J. E. Mueller, A.-C. Voigt, and J. M. Arrazola, *Quantum simulation of battery materials using ionic pseudopotentials*, [arXiv:2302.07981](#) [quant-ph].